GEOLOGY | THE GEOLOGICAL SOCIETY OF AMERICA®

https://doi.org/10.1130/G49015.1

Manuscript received 22 February 2021
Revised manuscript received 7 April 2021
Manuscript accepted 18 April 2021

© 2021 The Authors. Gold Open Access: This paper is published under the terms of the CC-BY license.

Published online 24 June 2021

Prior oil and gas production can limit the occurrence of injection-induced seismicity: A case study in the Delaware Basin of western Texas and southeastern New Mexico, USA

Noam Z. Dvory and Mark D. Zoback
Department of Geophysics, Stanford University, 397 Panama Mall, Stanford, California 94305, USA

ABSTRACT

We demonstrate that pore pressure and stress changes resulting from several decades of oil and gas production significantly affect the likelihood of injection-related induced seismicity. We illustrate this process in the Delaware Basin (western Texas and southeastern New Mexico, USA), in which hydraulic fracturing and waste-water injection have been inducing numerous earthquakes in the southernmost part of the basin where there has been no prior oil and gas production from the formations in which the earthquakes are now occurring. In the seismically quiescent part of the basin, we show that pore-pressure and poroelastic-stress changes associated with prior oil and gas production make induced seismicity less likely. The findings of this study have important implications for the feasibility of large-scale carbon storage in depleted oil and gas reservoirs.

INTRODUCTION

Understanding where and how anthropogenic processes that increase pore pressure at depth (waste-water injection, hydraulic fracturing, CO_2 injection, stimulation of geothermal wells, etc.) could potentially induce seismicity is important for seismic hazard mitigation. In this study, we show that while knowledge of the preexisting state of stress, pore pressure, and distribution of pre-existing faults enables one to predict the potential occurrence of induced seismicity, processes such as pore-pressure and stress changes associated with prior oil and gas production can significantly reduce the likelihood of induced seismicity. We investigate these phenomena in the Delaware Basin of western Texas and southeastern New Mexico (USA), where several studies link recent seismicity in the southernmost part of the basin to hydraulic fracturing and waste-water injection (e.g., Lomax and Savvaidis, 2019; Skoumal et al., 2020; Savvaidis et al., 2020). The Delaware Basin is the westernmost (and largest) part of the Permian Basin. Fluid injection associated with hydrocarbon development has long been suspected as triggering mechanisms for earthquakes at a number of sites in the Permian Basin since the 1960s (Rogers and Malkiel, 1979; Keller et al., 1981, 1987). The area also has occasional natural seismicity (Doser et al., 1991, 1992).

In much of the Delaware Basin, there has been hydrocarbon production from the Delaware Mountain Group (DMG) and Bone Spring Group (BSG) since the early 1970s. Figure 1A shows the distribution of production wells in the DMG, and Figure 1B shows the distribution of BSG production wells. Each of the four maps in Figure 1 shows the locations of 4482 earthquakes (red dots) recorded by the TexNet seismic network (http://coastal.beg.utexas.edu/texnetcatalog) since 2017 (Savvaidis and Hennings, 2020). Although the TexNet catalog does not report earthquakes outside Texas and the station coverage is much better in the southern part of the Delaware Basin, it is striking in Figures 1A and 1B that the parts of the basin where hydrocarbon production from the DMG and BSG has occurred are essentially free of triggered seismicity. Figures 1D and 1E show the areal and depth distributions of horizontal drilling and hydraulic fracturing operations throughout the Delaware Basin, principally in the Wolfcamp Group (WG), a Permian-age unconventional oil reservoir. More than 9000 horizontal wells have been drilled in the WG since 2014, each with multiple (typically 20–50) hydraulic fracturing stimulations. Figures 1C and 1F show the areal and depth distributions of waste-water injection wells, principally in the DMG, a sequence of Permian-age formations that includes several depleted conventional oil reservoirs in some areas. As is the case with WG production wells, waste-water injection wells are located throughout the basin. The water being injected includes saline water that flows back to the surface after hydraulic fracturing as well as water that is co-produced with oil. It is obvious in Figure 1 that the triggered seismicity in the Delaware Basin is highly concentrated in the southernmost part of the basin, despite the fact that horizontal drilling and multi-stage hydraulic fracturing and wastewater disposal are occurring throughout the basin. One objective of this study is to identify the processes that seem to prevent induced seismicity from occurring in areas of prior oil and gas production.

In our study, we do not address the mechanisms associated with the M 4.6 Mentone earthquake sequence of March 2020 (Savvaidis and Hennings, 2020), denoted by "M" in Figures 1A–1D. This earthquake sequence is spatially removed from the concentration of seismicity in Reeves and Pecos Counties (Texas) and appears to be associated with slip on deep, basement-rooted faults, possibly in response to waste-water injection at great depth occurring in that area. There are no deep injection wells in the area of seismicity in Reeves, Pecos, and Ward Counties (Texas) discussed here.

PORE PRESSURE AND STRESS

Lund Snee and Zoback (2018) used wellbore stress indicators and earthquake focal plane mechanisms to demonstrate that normal faulting characterizes the entire Delaware Basin and that the direction of maximum horizontal compression (S_{Hmax}) gradually rotates clockwise from being approximately north-south in the northern part of the basin, to approximately east-west at the border between New Mexico and Texas, to northwest-southeast in the southern part of the basin (black lines in Fig. 2A).

CITATION: Dvory, N.Z., and Zoback, M.D., 2021, Prior oil and gas production can limit the occurrence of injection-induced seismicity: A case study in the Delaware Basin of western Texas and southeastern New Mexico, USA: Geology, v. 49, p. 1198–1203, https://doi.org/10.1130/G49015.1

Downloaded from http://pubs.geoscienceworld.org/gsa/geology/article-pdf/49/10/1198/5413349/g49015.1.pdf by guest on 15 June 2026

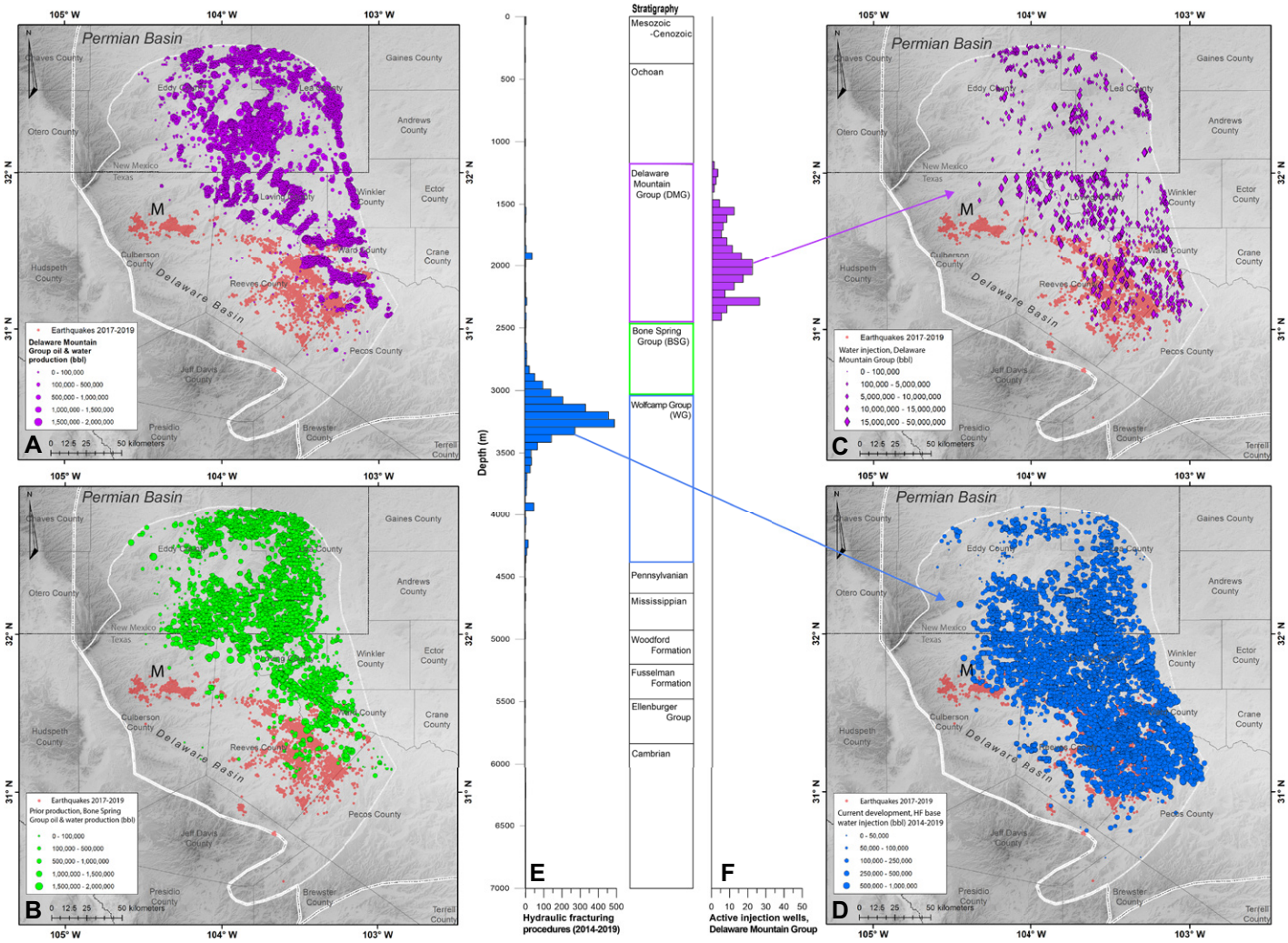

Figure 1. (A–D) Location of wells drilled in the Delaware Basin, western Texas and southeastern New Mexico (USA). Earthquake locations recorded by TexNet Seismic Monitoring Program (http://coastal.beg.utexas.edu/texnetcatalog) between 2017 and 2020 are shown with red dots. M is the location of the Mentone earthquake sequence. All production and injection values are in oilfield barrels (bbl). (A) Production wells in the Delaware Mountain Group (DMG) (purple dots). (B) Production wells in the Bone Spring Group (BSG) (green dots). (C) Waste-water injection wells in the DMG (purple dots). (D) Horizontal, multi-stage hydraulic fracturing (HF) wells in the Delaware Basin drilled between 2017 and 2020 (blue dots). (E) Depths of hydraulic fracturing operations in Reeves County (Texas) between 2017 and 2020. (F) Depths of waste-water injection wells in the DMG. Generalized stratigraphy in Reeves County is shown for reference in the center of the figure. Data are from FracFocus (https://fracfocus.org) and Enverus DrillingInfo (https://app.drillinginfo.com).

Correspondingly, focal mechanism data show that the orientation of fault planes rotates from north to south, consistently striking subparallel to the local direction of S_{Hmax}, as Coulomb faulting theory predicts.

Using a methodology that incorporates the uncertainties associated with the parameters utilized in Coulomb failure analysis (Walsh and Zoback, 2016), we colored faults in Figure 2A to indicate the pore pressure required for slip on basement faults mapped by Hennings et al. (2020) throughout the Delaware Basin and the surrounding areas. Figure 2B is an enlargement of the area near the boundary between Reeves and Pecos Counties. The earthquakes shown by black circles in Figure 2 represent relocated hypocentral depths (after Sheng et al., 2020). Before the Sheng et al. study, earthquake depths were poorly determined due to the sparseness of the TexNet network. Earthquake epicenters shown by gray dots in Figure 2B are from a relocation of a limited number of events (Savvaidis and Peng, 2020) using hypoDD software (Waldhauser, 2001) to produce highly accurate relative earthquake locations. Note that the earthquakes occur along lineations that trend northwest-southeast, parallel to S_{Hmax}, as expected in an area of normal faulting. The colored faults in Figure 2B again indicate the pore pressure required to induce fault slip, but in this figure panel we show only shallow faults, principally in the DMG (after Hennings et al.,2020). The blue lines in Figure 2B show interpolated and smoothed directions of maximum horizontal stress used in the Coulomb slip analysis, which used a continuously varying stress field and the methodology described by Carafa and Barba (2013) and Carafa et al. (2015). Figure 2B emphasizes the fact that lineations of seismicity, focal plane mechanisms, and mapped faults at shallow depth all indicate that the earthquakes in this area are being triggered on faults optimally oriented for slip in the local stress field.

Figure 3 presents a compilation of pore-pressure and stress data for the Reeves County area. As can be seen in Figure 3B, the detailed study of earthquake depths indicates that they are principally concentrated in the lower section of the DMG and the upper part of the BSG. The pore-pressure data in Figure 3A for Reeves County is principally from Luo et al. (1994), and the magnitude of the least principal stress, S_{hmin}, and the vertical stress, S_v, are from Smye et al. (2020). Both the pore pressure and stress state shown represent those that existed prior to hydraulic fracturing in the WG or waste-water injection into the DMG. S_{hmin} was determined

Downloaded from http://pubs.geoscienceworld.org/gsa/geology/article-pdf/49/10/1198/5413349/g49015.1.pdf by guest on 15 June 2026

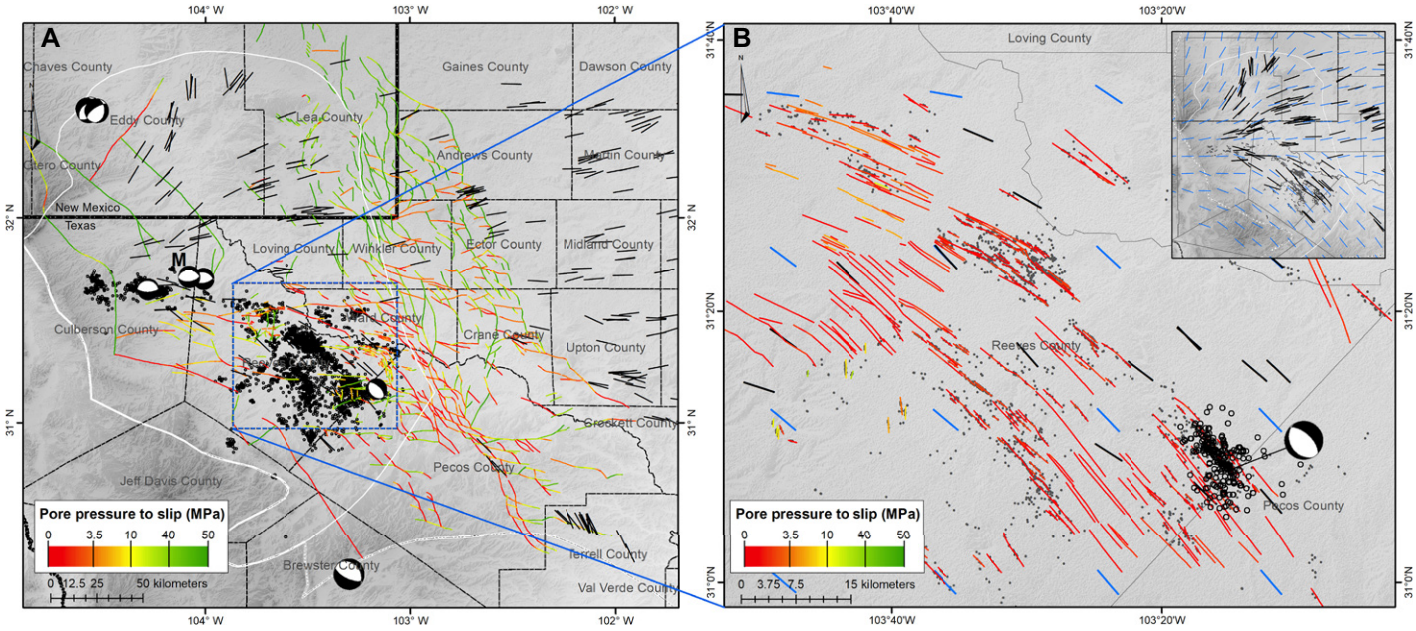

Figure 2. Pore pressure required for slip on basement faults and shallow faults. (A) Colored faults indicate pore pressure required for slip on basement faults in the Delaware Basin (western Texas and southeastern New Mexico (USA) mapped by Hennings et al. (2020). Direction of maximum horizontal principal stress is indicated by black lines. Earthquake epicenters (black circles) are from the TexNet Earthquake Catalog (http://coastal.beg.utexas.edu/texnetcatalog). M is the location of the Mentone earthquake sequence. Focal mechanisms are parallel to the S_{Hmax} orientation. (B) Earthquakes shown by black circles near the boundary between Reeves and Pecos Counties (Texas) are those for which relocated hypocentral depths are available. Earthquake epicenters shown by gray dots are from the TexNet relocation catalog of limited number of events utilizing hypoDD software (https://www.ldeo.columbia.edu/~felixw/hypoDD.html). Colored faults indicate pore pressure required for slip, principally in the Delaware Mountain Group (recently mapped by Hennings et al., 2020). Local indicators of direction of maximum horizontal stress are shown by black lines. Blue lines show interpolated and smoothed directions of maximum horizontal stress used in fault slip analysis in both figures (see text). Inset shows the smoothed stress orientation map that was used for the pore pressure to slip calculation.

from instantaneous shut-in pressures (ISIPs) associated with small-scale hydraulic fractures made specifically to determine S_{hmin}. Note that pore pressure is essentially hydrostatic in the DMG and BSG but increases markedly with depth in the upper part of the WG, defining what is sometimes referred to as a pressure ramp (e.g., Rittenhouse et al., 2016). Correspondingly, the magnitude of S_{hmin} increases suddenly with depth in the WG. This abrupt increase in the magnitude of S_{hmin} implies that hydraulic fractures associated with WG wells would be expected to propagate upward into the BSG where S_{hmin} is lower, an observation supported by microseismic events associated with wells hydraulically fractured in the upper WG (e.g., Parker et al., 2015).

Equation 1 can be used to estimate the value of S_{hmin} predicted by Coulomb faulting theory for optimally oriented normal faults in frictional failure equilibrium, where the coefficient of friction is designated by μ (see Jaeger and Cook, 1979) and P_P is the pore pressure:

$$S_{hmin} = \frac{S_V - P_P}{[(\mu^2 + 1)^{\frac{1}{2}} + \mu]^2} + P_P. \quad (1)$$

As shown by Zoback (2007), this equation accurately predicts the value of S_{hmin} in sedimentary basins characterized by normal faulting for a coefficient of friction (μ) of ~0.6. As indicated by the red straight line in Figure 3A, the value of S_{hmin} from Equation 1 accurately predicts observed values of the least principal stress in the BSG, further indicating that the BSG is in a state of frictional equilibrium. There are very few available measurements of S_{hmin} for the DMG in Reeves County. The four shallowest measurements are consistent with frictional equilibrium, while two measurements show higher values. The same is generally true in the WG—some of the S_{hmin} measurements are consistent with frictional equilibrium (using a simplification of the pore-pressure ramp as shown), but other measurements indicate higher values than that predicted by Equation 1. We suggest that the magnitude of S_{hmin} is higher than that predicted by frictional equilibrium because of viscoplastic stress relaxation in clay-rich lithofacies (Sone and Zoback, 2014), which reduces the difference between the maximum and minimum principal stress, S_v and S_{hmin}, respectively (see discussion in Zoback and Kohli, 2019). Viscoplastic creep of the WG shales has been documented in laboratory tests by Rassouli and Zoback (2020) who showed measurements of the least principal stress with depth in the WG that vary between being consistent with critically stressed normal faults in relatively low-clay lithofacies and significantly higher values in clay-rich lithofacies.

The Ochoan stratigraphic section above the DMG contains considerable evaporite deposits, resulting in a state of stress in which all three principal stresses are approximately equal. Consequently, it is not surprising that pore-pressure perturbations associated with either waste-water disposal or hydraulic fracturing operations occasionally trigger earthquakes in both the BSG and DMG. The shallow nature of the induced seismicity documented by Sheng et al. (2020) is consistent with the induced seismicity geomechanical mechanism presented here. Unfortunately, their results are limited to only a small area due to the relatively large station spacing of the TexNet array. Thus, further study of earthquake depths is required to thoroughly test the proposed induced seismicity mechanism.

POROELASTIC STRESS PATH ASSOCIATED WITH BONE SPRING GROUP PRODUCTION

The arguments in the previous sections focused on why seismicity could be triggered by waste-water injection in the DMG and/or hydraulic fracturing in the WG in the part of the Delaware Basin where there has been no prior production from either the DMG or the BSG. In this section, we discuss why seismicity is not occurring elsewhere in the Delaware Basin where production from the DMG and BSG occurred in the past. Because S_v is expected

Downloaded from http://pubs.geoscienceworld.org/gsa/geology/article-pdf/49/10/1198/5413349/g49015.1.pdf by guest on 15 June 2026

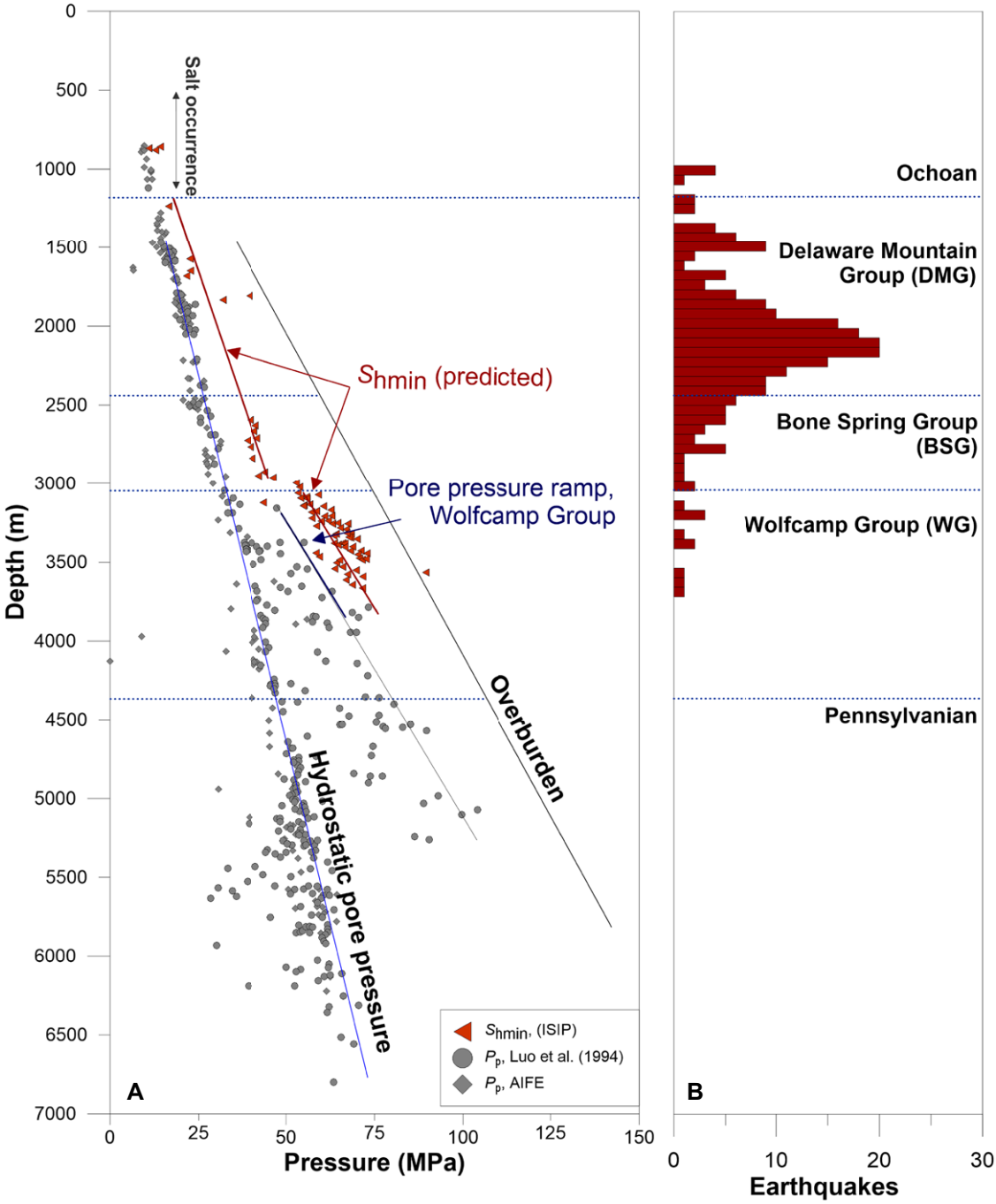

Figure 3. (A) Pore pressure, and measured least principal stress (S_{hmin}), as explained in the text. Hydrostatic pore pressure and estimated overburden stress are shown for reference. P_p—pore pressure, ISIP—instantaneous shut-in pressures test. AIFE relates to American Institute of Formation Evaluation (aife@cox.net). (B) Relocated earthquake depths near the boundary between Reeves and Pecos Counties (Texas) from Sheng et al. (2020).

to remain essentially constant during depletion of laterally extensive reservoirs (Segall and Fitzgerald, 1998), there is a reduction of the two horizontal stresses as P_p decreases due to production. The ratio of the stress change to pore pressure change is sometimes referred to as the stress path, A, given by:

$$A = \alpha \frac{1-2\nu}{1-\nu} = \frac{\Delta S_{Hor}}{\Delta P_p}, \quad (2)$$

where α is the Biot coefficient and ν is Poisson's ratio (Lorenz et al., 1991). S_{Hor} corresponds to both S_{Hmax} and S_{hmin} since the change in both horizontal stresses is expected to have the same linear correlation to the change in the pore pressure.

Figure 4 illustrates how pore pressure and stress evolve during depletion of the BSG reservoir from wells outside the seismically active area. This representation of stress and pore-pressure evolution with production as shown is based on the deformation analysis in reservoir space (DARS) representation of Chan and Zoback (2002). In Figure 4, Equation 1 is represented by the diagonal solid line, normalized by S_v so that data from different wells (where the BSG is at slightly different depths) can be shown together in the same figure. In other words, this line represents how the magnitude of S_{hmin} varies as a function of pore pressure for a reservoir in a state of normal faulting frictional equilibrium (assuming $\mu = 0.6$). At any given pore pressure, if the magnitude of S_{hmin} is on this line, well-oriented normal faults are in a state of frictional faulting equilibrium. This is indicated by the green diamonds, which are equivalent to the data points for the BSG shown in Figure 3A. Data points that plot above this line indicate a stable stress state, which would require an increase in P_p (shifting the point to the right) to hit the failure line and induce slip. It is generally recognized that the change in the magnitude of the least principal stress with depletion in normal-faulting areas tends to suppress the

Downloaded from http://pubs.geoscienceworld.org/gsa/geology/article-pdf/49/10/1198/5413349/g49015.1.pdf by guest on 15 June 2026

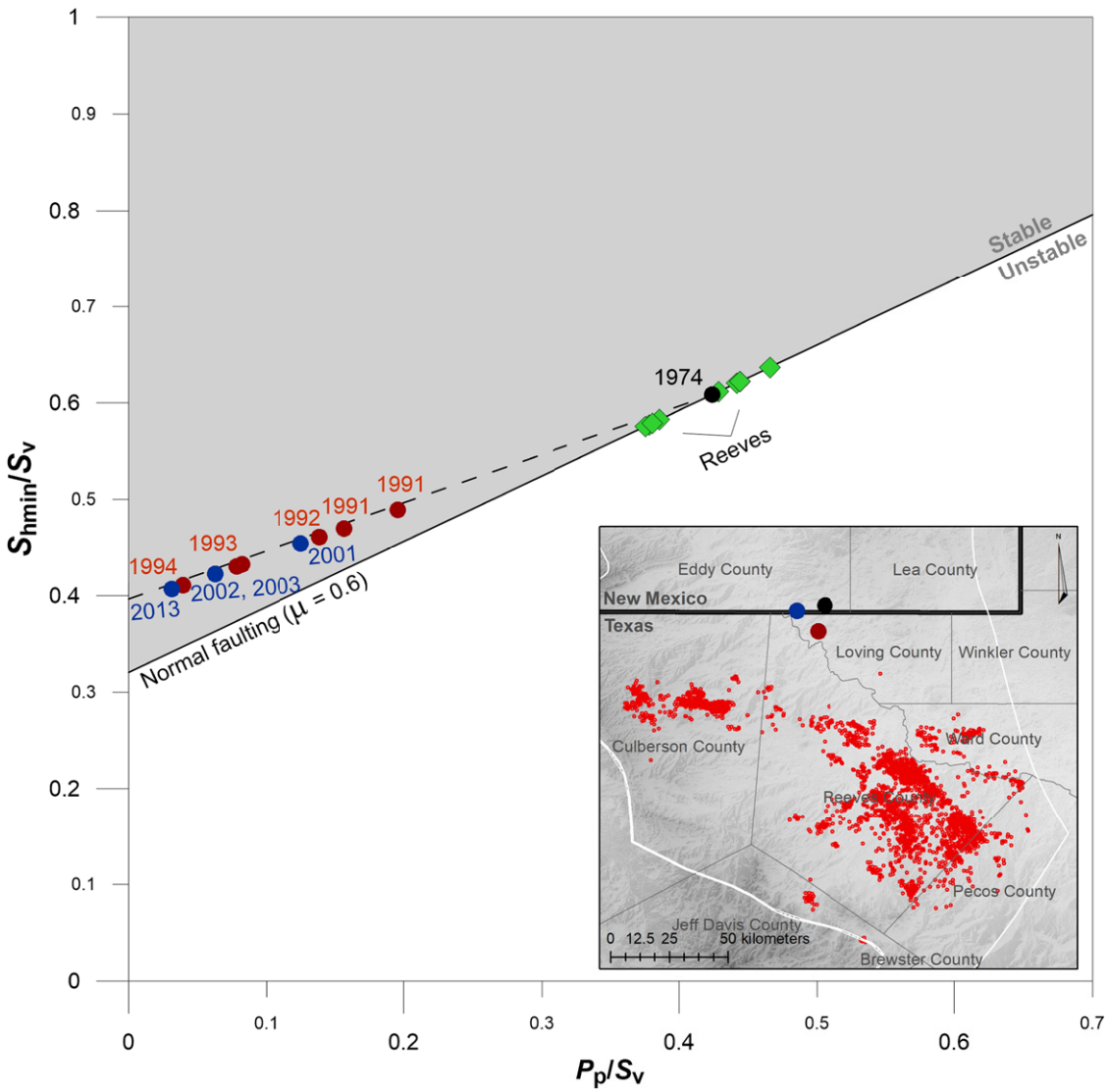

Figure 4. Evolution of the state of stress in "reservoir space" in terms of pore pressure (P_p) and least principal stress (S_{hmin}), shown normalized by overburden stress, S_v. μ is the friction coefficient, and the solid line represents frictional failure equilibrium. If the reservoir stress state is below the solid line, then it is unstable and induced seismicity might occur. Dashed line represents the stress path, in the case presented here, the poroelastic response to the reservoir depletion moves the stress state of the reservoir away from frictional failure equilibrium conditions and toward a stable state where induced seismicity is less likely to occur. Map shows locations of wells corresponding to pore-pressure data points shown with the same color (larger blue, red, and black dots, shown in plot labeled with year of measurement). The smaller red dots are earthquake locations from the TexNet catalog (http://coastal.beg.utexas.edu/texnetcatalog), and the white lines are the Delaware basin boundaries. Green diamonds show stress and correlated pore pressure in wells in the Bone Spring Group (BSG) in Reeves County (Texas) where there has been no depletion of the Bone Spring reservoir.

tendency for normal faulting (see discussion in Zoback, 2007).

Pore-pressure measurements for the BSG at different times are available for three wells in Eddy (New Mexico) and Loving (Texas) Counties just to the north of the area of triggered seismicity, at the locations shown by the black, red, and blue dots in the inset map in Figure 4. The red and blue dots in Figure 4 show the values of pore pressure at various times and S_{hmin} values based on an assumed stress path, A, of 0.5 (Equation 2). Chan and Zoback (2002) present data for a number of depleted oil and gas fields that indicate stress paths of 0.5–0.6. Because depletion normally moves the stress state away from normal faulting, the representation of pore pressure and stress in Figure 4 indicates why seismicity is not occurring where BSG production has occurred. If we use appropriate values of S_v for the wells shown, the depletion-induced decrease in pore pressure in the BSG in 2013 was so large that it would require a significant pressure increase of 6.2 MPa to trigger normal faulting, even on the most optimally oriented faults.

CONCLUSIONS

In the seismically active Reeves County–Pecos County area, potentially active normal faults trend NW-SE, parallel to the direction of maximum horizontal compression in that area. Hydraulic fracturing and waste-water disposal appear to be triggering slip on northwest-southeast–trending normal faults in the DMG and BSG in the part of the Delaware Basin where these faults were at frictional equilibrium at the initiation of horizontal drilling and multi-stage hydraulic fracturing activities in the WG and waste-water injection in the DMG. Elsewhere in the Delaware Basin, poroelastic stress changes result in a stress state that makes induced seismicity less likely. Analyses such as this will be essential in evaluating the potential for long-term sequestration of CO_2 in depleted oil and gas reservoirs and thoroughly evaluating potential seismic hazards.

ACKNOWLEDGMENTS

The Stanford Center for Induced and Triggered Seismicity (Stanford, California, USA) funded this work. We thank Bill Ellsworth and Peter Hennings for helpful conversations. Well data were obtained from the Enverus DrillingInfo database (https://app.drillinginfo.com), FracFocus (https://fracfocus.org), Steven Misner of AIFE (aife@cox.net), and the Texas Railroad Commission (http://rrc.texas.gov). Earthquake data were obtained from the TexNet database (http://coastal.beg.utexas.edu/texnetcatalog). We also thank the GEOLOGY Science Editor, Marc Norman, and the reviewers Jeff Nunn and Steve Willson for their important comments.

REFERENCES CITED

Carafa, M.M.C., and Barba, S., 2013, The stress field in Europe: Optimal orientations with confidence limits: Geophysical Journal International, v. 193, p. 531–548, https://doi.org/10.1093/gji/ggt024.

Carafa, M.M.C., Tarabusi, G., and Kastelic, V., 2015, SHINE: Web application for determining the horizontal stress orientation: Computers & Geosciences, v. 74, p. 39–49, https://doi.org/10.1016/j.cageo.2014.10.001.

Chan, A.W., and Zoback, M.D., 2002, Deformation Analysis in Reservoir Space (DARS): A simple

Downloaded from http://pubs.geoscienceworld.org/gsa/geology/article-pdf/49/10/1198/5413349/g49015.1.pdf by guest on 15 June 2026

formalism for prediction of reservoir deformation with depletion: Paper SPE-78174-MS presented at SPE/ISRM Rock Mechanics Conference, Irving, Texas, 20–23 October, https://doi.org/10.2523/78174-ms.

Doser, D.I., Baker, M.R., and Mason, D.B., 1991, Seismicity in the War-Wink gas field, Delaware Basin, west Texas, and its relationship to petroleum production: Bulletin of the Seismological Society of America, v. 81, p. 971–986.

Doser, D.I., Baker, M.R., Luo, M., Marroquin, P., Ballesteros, L., Kingwell, J., Diaz, H.L., and Kaip, G., 1992, The not so simple relationship between seismicity and oil production in the Permian Basin, west Texas: Pure and Applied Geophysics, v. 139, p. 481–506, https://doi.org/10.1007/BF00879948.

Hennings, P., Dvory, N.Z., Horne, E., and Zoback, M.D., 2020, Slip potential and seismogenic association of basement-rooted faults in the Delaware Basin, West Texas: Abstract S013-0011 presented at American Geophysical Union Fall Meeting, 1–17 December 2020.

Jaeger, J.C., and Cook, N.G.W., 1979, Fundamentals of Rock Mechanics (third edition): New York, Chapman and Hall, 593 p.

Keller, G.R., Rogers, A.M., Lund, R.J., and Orr, C.D., 1981, A seismicity and seismotectonic study of the Kermit seismic zone, Texas: U.S. Geological Survey Open-File Report 81-37, 388 p., https://doi.org/10.3133/ofr8137.

Keller, G.R., Rogers, A.M., and Orr, C.D., 1987, Seismic activity in the Permian Basin area of West Texas and southeastern New Mexico, 1975–79 (USA): Seismological Research Letters, v. 58, p. 63–70, https://doi.org/10.1785/gssrl.58.2.63.

Lomax, A., and Savvaidis, A., 2019, Improving absolute earthquake location in west Texas using probabilistic, proxy ground-truth station corrections: Journal of Geophysical Research: Solid Earth, v. 124, p. 11,447–11,465, https://doi.org/10.1029/2019JB017727.

Lorenz, J.C., Teufel, L.W., and Warpinski, N.R., 1991, Regional fractures I: A mechanism for the formation of regional fractures at depth in flat-lying reservoirs: American Association of Petroleum Geologists Bulletin, v. 75, p. 1714–1737, https://doi.org/10.1306/0c9b29e3-1710-11d7-8645000102c1865d.

Lund Snee, J.E., and Zoback, M.D., 2018, State of stress in the Permian Basin, Texas and New Mexico: Implications for induced seismicity: The Leading Edge, v. 37, p. 127–134, https://doi.org/10.1190/tle37020127.1.

Luo, M., Baker, M.R., and LeMone, D.V., 1994, Distribution and generation of the overpressure system, eastern Delaware Basin, western Texas and southern New Mexico: American Association of Petroleum Geologists Bulletin, v. 78, p. 1386–1405, https://doi.org/10.1306/A25FECB1-171B-11D7-8645000102C1865D.

Parker, J., Bazan, L.W., Tran, V.P., White, R., and Latibeaudiere, M.G., 2015, Technology integration: A methodology to enhance production in horizontal Wolfcamp shale wells in the Delaware basin: Paper SPE-175535-MS presented at Society of Petroleum Engineers Liquids-Rich Basins Conference—North America, Midland, Texas, 2–3 September, https://doi.org/10.2118/175535-ms.

Rassouli, F.S., and Zoback, M.D., 2020, Preliminary results on multi-stage creep experiments of the Wolfcamp Shale at elevated temperature: Paper ARMA-2020-1577 presented at 54th U.S. Rock Mechanics/Geomechanics Symposium, virtual, 28 June–1 July.

Rittenhouse, S., Currie, J., and Blumstein, R., 2016, Using mud weights, DST, and DFIT data to generate a regional pore pressure model for the Delaware Basin, New Mexico and Texas: Paper 2450423 presented at 4th Unconventional Resources Technology Conference, San Antonio, Texas, 1–3 August, https://doi.org/10.15530/urtec-2016-2450423.

Rogers, A.M., and Malkiel, A., 1979, A study of earthquakes in the Permian Basin of Texas–New Mexico: Bulletin of the Seismological Society of America, v. 69, p. 843–865.

Savvaidis, A., and Hennings, P., 2020, Preliminary report on the M4.9 Earthquake in Culberson-Reeves County Line, M4.9-Culberson-Reeves_County_Line-Earthquake-20200326: Texas Data Repository, https://doi.org/10.18738/T8/VHKAXV.

Savvaidis, A., and Peng, L., 2020, TexNet earthquake hypoDD cross correlation relocation catalog of Permian Basin from 20170101 to 20200930: Texas Data Repository, https://doi.org/10.18738/T8/RBEGTH.

Savvaidis, A., Lomax, A., and Breton, C., 2020, Induced seismicity in the Delaware Basin, West Texas, is caused by hydraulic fracturing and wastewater disposal: Bulletin of the Seismological Society of America, v. 110, p. 2225–2241, https://doi.org/10.1785/0120200087.

Segall, P., and Fitzgerald, S.D., 1998, A note on induced stress changes in hydrocarbon and geothermal reservoirs: Tectonophysics, v. 289, p. 117–128, https://doi.org/10.1016/S0040-1951(97)00311-9.

Sheng, Y., Ellsworth, W.L., and Pepin, K.S., 2020, On the depth of earthquakes in the Delaware Basin—A case study along the Reeves-Pecos County line: Abstract S013-0007 presented at American Geophysical Union Fall Meeting, 1–17 December 2020.

Skoumal, R.J., Barbour, A.J., Brudzinski, M.R., Langenkamp, T., and Kaven, J.O., 2020, Induced seismicity in the Delaware Basin, Texas: Journal of Geophysical Research: Solid Earth, v. 125, e2019JB018558, https://doi.org/10.1029/2019JB018558.

Smye, K.M., Hennings, P.H., and Horne, E.A., 2020, Variations in vertical stress in the Permian Basin Region: American Association of Petroleum Geologists Bulletin, https://doi.org/10.1306/10092019189 (in press).

Sone, H., and Zoback, M.D., 2014, Viscous relaxation model for predicting least principal stress magnitudes in sedimentary rocks: Journal of Petroleum Science Engineering, v. 124, p. 416–431, https://doi.org/10.1016/j.petrol.2014.09.022.

Waldhauser, F., 2001, hypoDD: A computer program to compute double-difference hypocenter locations: U.S. Geological Survey Open File Report 2001-113, 25 p., https://doi.org/10.3133/ofr01113.

Walsh, F.R., III, and Zoback, M.D., 2016, Probabilistic assessment of potential fault slip related to injection-induced earthquakes: Application to north-central Oklahoma, USA: Geology, v. 44, p. 991–994, https://doi.org/10.1130/G38275.1.

Zoback, M.D., 2007, Reservoir Geomechanics: Cambridge, UK, Cambridge University Press, 452 p., https://doi.org/10.1017/CBO9780511586477.

Zoback, M.D., and Kohli, A.H., 2019, Unconventional Reservoir Geomechanics: Cambridge, UK, Cambridge University Press, 484 p., https://doi.org/10.1017/9781316091869.

Printed in USA

Downloaded from http://pubs.geoscienceworld.org/gsa/geology/article-pdf/49/10/1198/5413349/g49015.1.pdf by guest on 15 June 2026